Properties of r.f. sputtered cadmium telluride thin films

M. MARAFI, F. EL AKKAD, B. PRADEEP
Physics Department, Kuwait University, P.O. Box 5969, Safat 13060, Kuwait

CdTe thin films were prepared using r.f. magnetron sputtering in an Ar atmosphere. Substrate temperatures in the range 100–320 °C were used. XRD results showed that the films are amorphous below 200 °C while above 200 °C the firms were polycrystalline with cubic structure and grains preferentially oriented along the [1 1 1] crystallographic direction. SEM measurements showed significant enhancement of crystallite size with increase of T_s or with post-preparation annealing above 400 °C. The 5 K photoluminescence spectrum showed a broad (FWHM = 80 meV) band with a maximum at 1.538 eV. This band showed significant narrowing after annealing above 400 °C suggesting that it originates from transitions involving grain boundary defects. The refractive index n was determined from the interference pattern of the optical transmission. The results agree with the values of n calculated using the Jensen theory. The absorption coefficient was determined for photon energies $h\nu \geq E_g$ (the energy bandgap) from the optical transmission spectra in the absorption region using the Swanepoel theory. Several direct and indirect allowed optical transitions were identified. It was found that the transitions can be grouped into four main allowed transitions (two direct; E_o, E_3 and two indirect; E_1, E_2) whose energy values vary from one sample to another due the quantum size effect associated with small grain size. The main transitions are: E_o (1.50–1.77 eV) assigned to Γ_8 valence band (VB) $\rightarrow \Gamma_6$ conduction band (CB) transition, E_1 (1.84–2.05 eV) assigned to $L_{4,5}$(VB) $\rightarrow \Gamma_i$ transition where Γ_i is an impurity level at 1.2 eV above the Γ_8 (VB), E_2 (2.37–2.49 eV) assigned to $L_{4,5}$ (VB) $\rightarrow \Gamma_6$ (CB) transition and E_3 (2.25–2.55 eV) assigned to Γ_7 (VB) $\rightarrow \Gamma_i$ transition. The impurity is attributed to native centers or grain-boundary-related defects.

1. Introduction

In the past decade, considerable interest has been shown in the study of CdTe due to its importance as a material for optoelectronic applications, particularly in the field of polycrystalline thin-film solar cells. A number of techniques have been used for the preparation of such films [1, 2] and all-thin-film solar cells have been prepared with an efficiency of 15.8% [3] using hetero-junctions of the type CdTe/CdS prepared by closed-space sublimation. On the other hand, the cells prepared by r.f. sputtering are relatively less well, studied despite the known importance of r.f. sputtering as a suitable technique for large-scale applications. The efficiency of all-sputtered CdTe/CdS cells has reached 12.4% [4]. A further improvement of the efficiency requires detailed studies of the physical properties of the material in the thin-film form.

The optical properties of CdTe single crystals and thin films have been reported in the literature [5–8]. However, there have been no reports on the refractive index of r.f. sputtered thin films. Also, the optical transitions in this type of films have not been studied in detail. Here, we report on the optical properties of r.f. sputtered CdTe thin films. The refractive index was determined and the experimental values compared with those calculated using the Jensen theory [8] for the refractive index of semiconductors below the bandgap energy. Also, we present a detailed analysis of the optical absorption results, which reveal four main optical transitions (two direct and two indirect) in the energy range 1.50–2.50 eV in this type of films.

2. Experimental

CdTe thin films were prepared using r.f. magnetron, sputtering in an Ar atmosphere. Substrate temperatures between 100 and 320° and an r.f. power of 80 W were used. A hot-pressed CdTe target (purity 99.999%) from E-Vac Inc. was used. The sputtering was performed in the chamber of a Edward 306 sputtering system, which uses a planar magnetron source. A base pressure of 1.3×10^{-3} Pa was reached before admitting pure Ar gas (99.999%) at a pressure of about 0.67 Pa. More details on experimental procedure have been given elsewhere (see, for example, El Akkad *et al*. [9]).

The film thicknesses were measured using a Tencor Instruments profiler type Alpha-Step 200. Transmission measurements were carried out in the wavelength range

$300 \leq \lambda \leq 3000$ nm using a Cary 5E spectrophotometer. For XRD spectra, an X-ray diffractometer, Siemens D5000, was used.

The luminescence was excited using a CW argon ion laser of intensity 80 mW focused to 1.55 mm^2. Lock-in detection was performed. PMT with a GaAs : Cs cathode, spectrally flat up to 850 nm, and a grating monochromator were used.

3. Results and discussion

3.1. Structural and luminescence properties

For substrate temperatures $T_s \leq 200\,^{\circ}C$, the XRD pattern (Fig. 1) is featureless indicating that the range of crystallinity of the films is less than a hundred angstroms [10, 11]. These films are likely to have an amorphous nature. For temperatures $T_s > 200\,^{\circ}C$, the XRD spectra indicate a cubic CdTe structure with preferential crystallite orientation along the [1 1 1] crystallographic direction.

The effect of annealing on the crystallinity of the films is demonstrated in Fig. 2, which shows two SEM pictures for a CdTe film sputter-deposited on a steel substrate at 100 °C before and after annealing at 450 °C for 15 min. While before annealing no crystallite domains could be observed, the domains grow to a size ranging from 300 to 1000 nm after annealing.

The photoluminescence spectra at 5 K for the film before and after annealing are shown in Fig. 3. Before annealing, a broad band (full width at half maximum FWHM = 80 meV) with a peak at 1.538 eV is observed.

This band becomes much narrower (FWHM = 22 meV) with no measurable change in peak position after annealing. The significant narrowing of the band with the growth of grains after annealing suggests that it involves transitions associated with grain-boundary defects.

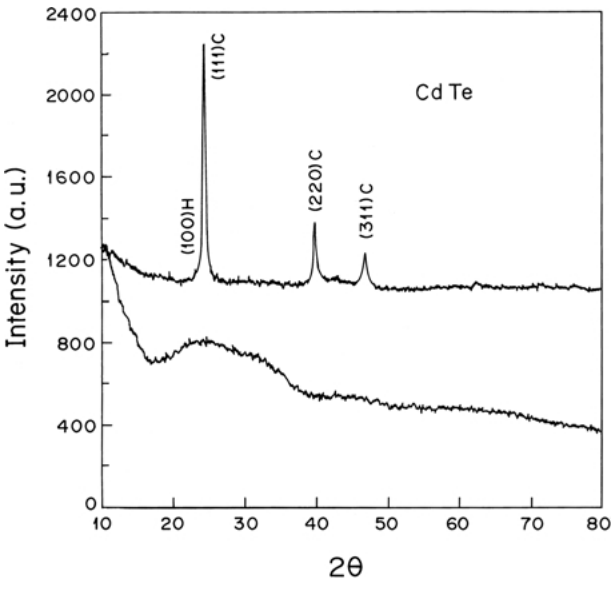

Figure 1 Typical XRD spectra for amorphous (lower spectrum) and polycrystalline (upper spectrum) films of r.f. sputtered CdTe.

3.2. Optical properties

3.2.1. Refractive index

The optical transmission was measured in the wavelength range $300 \geq \lambda \geq 3000$ nm. Typical results are shown in Fig. 4. The refractive index n can be calculated from the interference fringes appearing at long wavelengths using the basic equation for those fringes

$$2nd = m\lambda$$

where m is an integer for maxima and half integer for minima. The sample thickness d was measured using the Tencor profiler and was precise to 3%. Fig. 5 shows the experimental values of n as a function of photon energy for some representative samples.

The refractive index n was calculated using the following equation derived theoretically by Jensen [8] for compound semiconductors below the energy band gap.

$$n^2 = 1 + 2C_o[(y_B - y_F) - z(\tan^{-1}(y_B/z) - \tan^{-1}(y_F/z))] \quad (1)$$

where

$$C_o = \frac{R}{E_o^2} \quad (2)$$

R being a constant, and E_o the energy band gap (1.46 eV for CdTe single crystals [7]), and

$$z = \left(1 - \frac{h\nu}{E_o}\right)^{1/2} \quad (3)$$

$$y_B = M(a_o - a) \quad (4)$$

$$y_F = \frac{1}{2}\left(\frac{m_n}{m_r}\right)^{1/2} \lambda_c k_F \quad (5)$$

where M and a_o are constants (for the II–VI compounds $M = 3.46 \pm 0.2\,nm^{-1}$, $a_o = 1.737 \pm 0.088$ nm), and a is the lattice constant. $k_F = (3\pi^2 n_c)^{1/3}$ is the electron wave vector at low carrier concentration n_c.

$$\lambda_c = \left(\frac{n^2}{2m_n E_o}\right)^{1/2}$$

m_n is the electron effective mass, m_r is the reduced effective mass of electrons and holes (for CdTe $m_n \simeq m_r$).

Fig. 5 shows the calculated values of n as a function of $h\nu$ (solid line). The values of parameters used are $a_o = 1.825$ nm, $M = 3.66\,nm^{-1}$, $a = 0.641$ nm, $y_F = 0.203/E_o^{1/2}$ for $n_c = 10^{15}\,cm^{-3}$ (the calculated value of n does not show significant variation with y_F for values of n_c between 10^{14} and $10^{17}\,cm^{-3}$), $C_o = 1.12$ [8]. It is seen in Fig. 4 that, within experimental uncertainty of about 5%, the calculated values of n account fairly well for the observed values.

3.2.2. Absorption coefficient

The absorption coefficient α was calculated from T in the region of the strong absorption ($\lambda \leq 840$ nm) where the interference fringes disappear. In this case, according to Swanepoel [12], the following equation holds for an absorbing film on a transparent substrate,

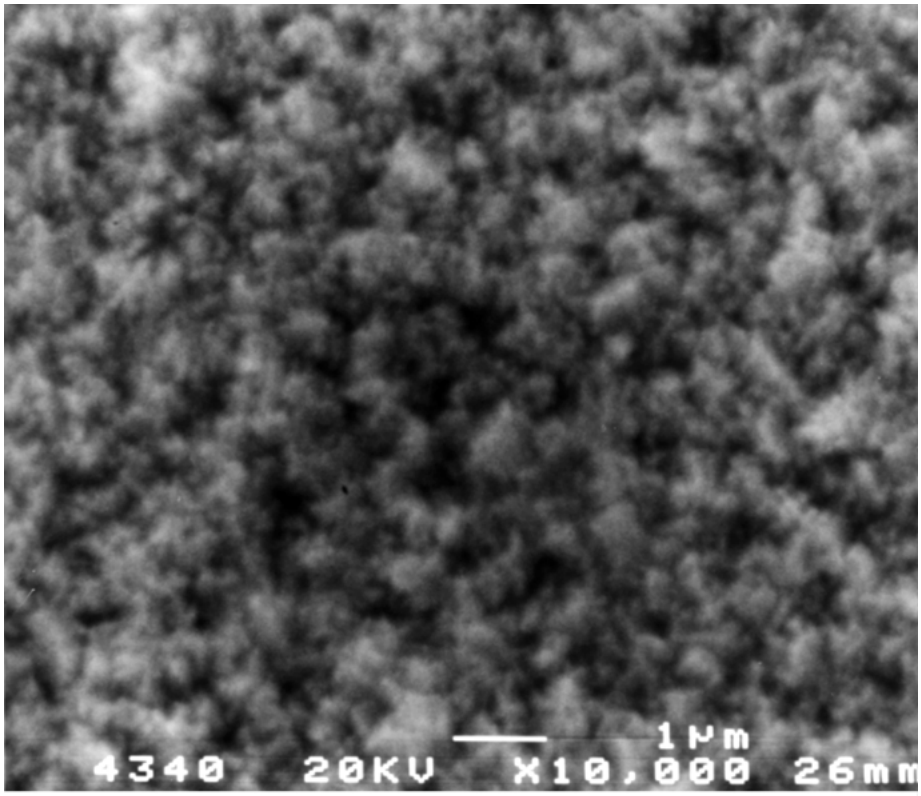

(a)

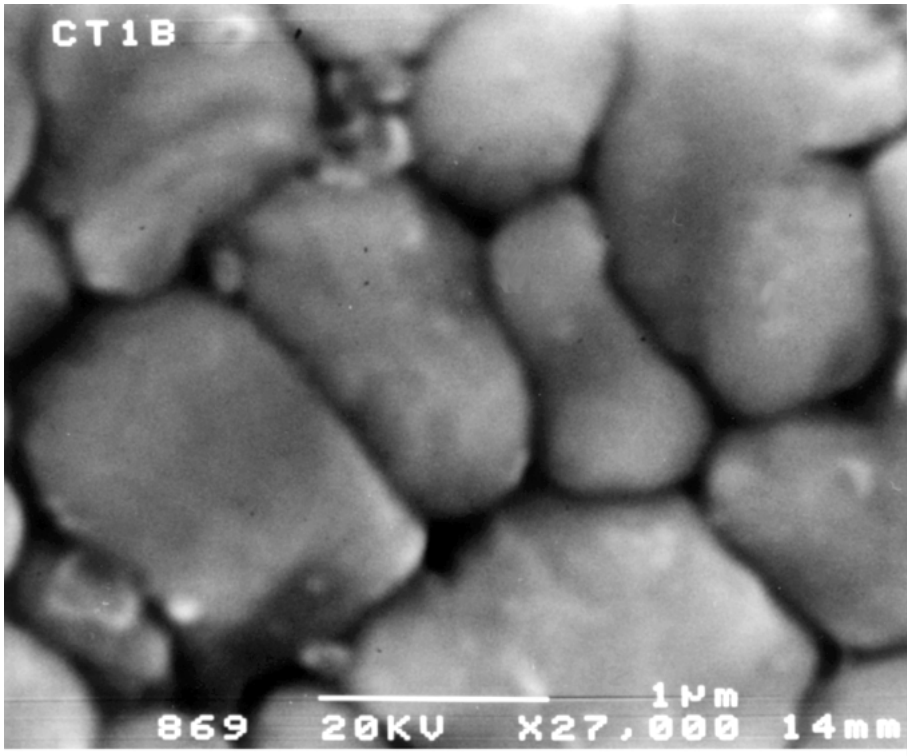

(b)

Figure 2 SEM pictures of a CdTe film deposited on steel with substrate temperature of 100 °C (a) before and (b) after annealing in air at 450 °C for 15 min.

$$x = \frac{(n+1)^3(n+s^2)}{16n^2s}T \qquad (6)$$

where $x = \exp(-\alpha d)$ and s is the refractive index of the glass substrate $(s = 1.53)$. The values of n as a function of photon energy were obtained by extrapolation from the lower photon energy range (Fig. 5).

The observed value of α is a result of the contribution of several optical transitions so that $\alpha(h\nu) = \Sigma\alpha_i(h\nu)$ $(i = 0,1,2 \ldots \text{etc.})$, where the values of i designate different transitions. The various contributions $\alpha_i(h\nu)$ can be calculated since usually different optical transitions dominate over different photon energy ranges. The procedure of separating $\alpha_i(h\nu)$ is as follows: there is a linear relationship between $(\alpha_i h\nu)^l$ and $h\nu$ where $l = 2$ and 1/2 for direct and indirect allowed

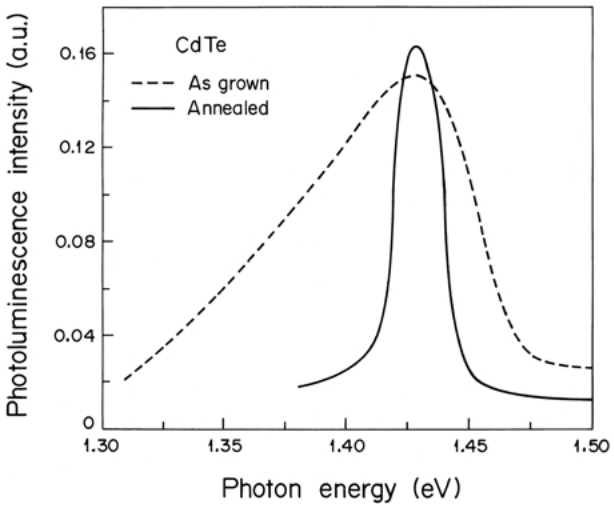

Figure 3 Luminescence spectrum at 5 K for r.f. sputtered CdTe film prepared at $T_s = 100\,^{\circ}$C: (- - -) before annealing, (—) after annealing, at 450 °C for 15 min.

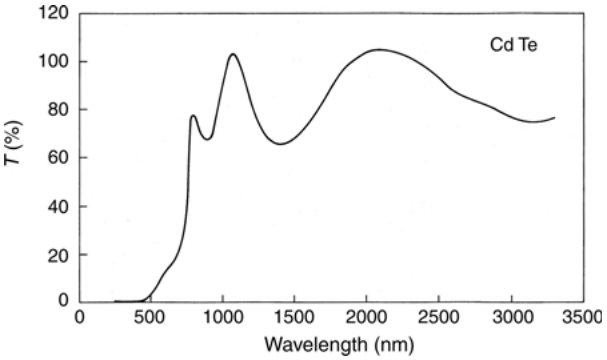

Figure 4 Optical transmission as a function of wavelength for a CdTe thin film of thickness 466 nm.

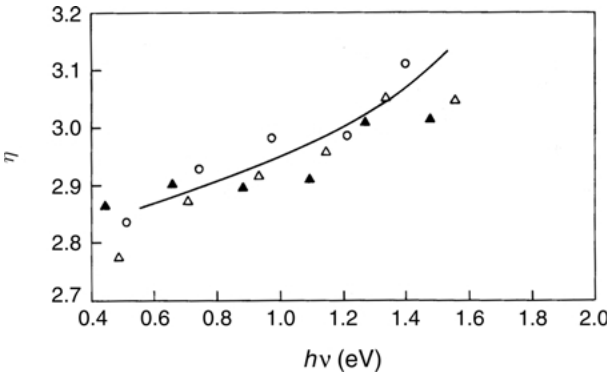

Figure 5 Refractive index n as a function of photon energy $h\nu$ for some representative samples of r.f. sputtered CdTe thin films prepared at 250 °C (open triangles), 300 °C (circles), annealed at 400 °C (solid triangles). Solid line: computed curve of n versus $h\nu$ using the Jensen theory [8].

transitions, respectively [13, 14]. Therefore, by plotting $(\alpha h\nu)^l$ against $h\nu$ one may obtain, over a given range of photon energy, a straight line described by

$$(\alpha_0 h\nu)^l = A_o + B_o h\nu \tag{7}$$

The first transition energy E_o is then determined from the intersection of the line with the $h\nu$ axis,

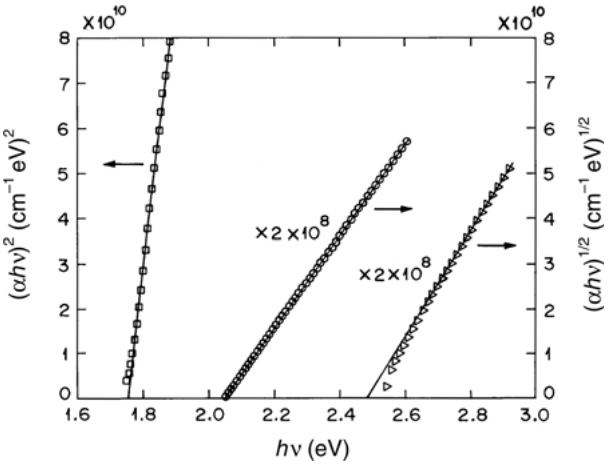

Figure 6 $(\alpha h\nu)^l (1 = 2 \text{ or } \frac{1}{2})$ against photon energy $h\nu$ for a CdTe thin film prepared at substrate temperature of 100 °C, showing E_o, E_1 and E_2 transitions.

$$E_0 = -\frac{A_o}{B_o} \tag{8}$$

Once a straight line is obtained, the values of $(\alpha_0 h\nu)^l$ are extrapolated to the higher photon energy range, then $\alpha_o(h\nu)$ is subtracted from the values of $\alpha(h\nu)$ in this range. A second plot $(\alpha h\nu)^l$ versus $h\nu$ is then constructed and the above procedure is repeated to find E_1 from the new straight line. The next value of E_i is found in the same way.

Fig. 6 shows the $(\alpha h\nu)^l$ versus $h\nu$ plots for a representative sample. The values of E_i obtained for a number of samples are given in Table I. Two direct (E_o, E_3) and two indirect (E_1, E_2) allowed transitions are revealed. Fig. 7 shows a plot of $(\alpha_o h\nu)^2$ against $h\nu$ for an

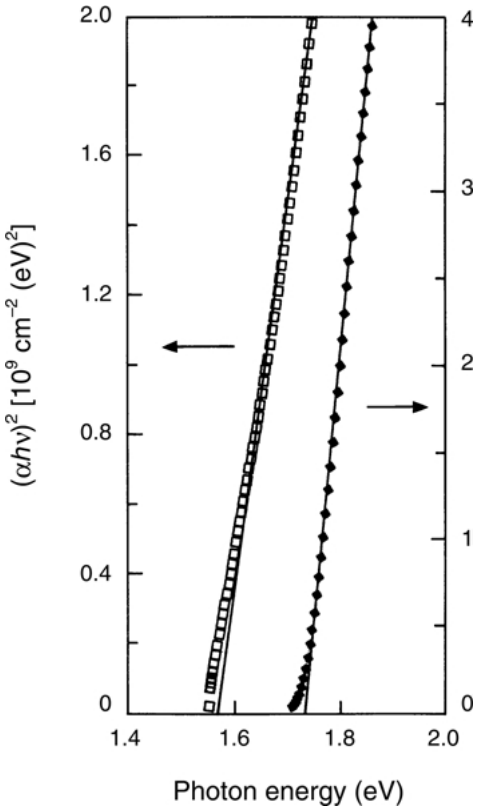

Figure 7 plot of $(\alpha h\nu)^2$ against $h\nu$ for r.f. sputtered CdTe thin films: (◆) Prepared at substrate temperature of 150 °C. (□) Annealed at 400 °C for 30 min.

TABLE I Optical transitions determined from absorption data for some CdTe thin films

Sample	T (°C)	E_o^d (eV)	E_1^i (eV)	E_2^i (eV)	E_3^d (eV)
5au	100[s]	1.775	2.051	2.485	
2b	150[s]	1.714			
3b	200[s]	1.655	1.897	2.370	
4b	250[s]	1.624			2.417
5b	300[s]	1.614			
6b	320[s]	1.632	1.970		2.549
5ba	400[a]	1.547	1842		
5aa	450[a]	1.502			2.250

s = substrate temperature, a = annealing tempertature, d = direct, i = indirect.

as-grown sample prepared at $T_s = 150\,^{\circ}\mathrm{C}$ and sample annealed at 400 °C for 30 min. It is shown that the value of the energy bandgap E_o is higher before annealing (1.714 eV before and 1.547 eV after annealing). It has been found that the energy bandgap E_o exhibits an enlargement that increases as the preparation temperature decreases (Table I). Fig. 8 shows the change ΔE_0 in the energy bandgap as a function of substrate temperature T_s ($\Delta E_o = E_o - E_g$ where $E_g = 1.46\,\mathrm{eV}$ is the bandgap of CdTe [7]).

The behavior of ΔE_o with T_s (Fig. 8) can be related to quantum size effects. The microcrystalline nature of the films (with average grain sizes or column diameter ≤ 10 nm and grain-boundary barriers) can be the origin of electron confinement, resulting in quantum states in the valence and conduction bands that would open the gap. This effect has been suggested in a study of CdSe films with small grain size [15] and has been treated theoretically by Melendez-Lira *et al*. [16] for films exhibiting columnar growth, as is the case for CdTe films. In this case, ΔE_o is given by

$$\Delta E_o = \frac{N}{A} \tag{9}$$

where A is the area of the column cross-section, assumed to be in the form of a wire, and N is a constant, which depends on the shape of the wire's cross-section (square, circular, etc.). Assuming that the growth of the grains is thermally activated, the column area can be written in the form

$$A = A_o \exp\left(-\frac{\Delta E_c}{kT_s}\right) \tag{10}$$

where ΔE_c is an activation energy associated with the columnar growth process.

From Equations 9 and 10 one obtains,

$$\Delta E_o = N \exp\left(\frac{\Delta E_c}{kT_s}\right) \tag{11}$$

The solid line in Fig. 8 is the best fit to the experimental data using the above equation, which yields $N = 1.70 \times 10^{-2}$ eV, $\Delta E_c = 0.16$ eV. It is shown that the experimental values of ΔE_o can be fairly well accounted for using Equation 11. This suggests that quantum size effects are the dominant cause of enlargement of E_o in our samples. This implies that the domains in Fig. 2 are not single grains.

Fig. 9 shows the transition energies E_1, E_2, and E_3 as a function of E_o. It is seen that the energy values of E_1, E_2, and E_3 increase with the increase of E_o suggesting that the same effect is responsible for the energy variation for all transitions. The extrapolation to $E_o = 1.460$ eV (bandgap energy of CdTe single crystals) yields the transition energies expected for CdTe single crystals: $E_1 = 1.770 \pm 0.089$ eV (indirect), $E_2 = 2.170 \pm 0.220$ eV (indirect), $E_3 = 2.175 \pm 0.109$ eV (direct).

E_o is attributed to the transition $\Gamma_8(\mathrm{VB}) \rightarrow \Gamma_6(\mathrm{CB})$. However, the Γ_6(CB) should be located at 1.46 eV instead of 1.59 eV above the Γ_8(VB), the latter value being calculated by Chelikowsky and Cohen [17]. On the other hand, an indirect transition at 2.13 eV (close to $E_2 = 2.17$ eV) was observed previously in single crystals [7]. The energy of that transition agrees with that (2.11 eV) of the interband transition $\mathrm{L}_{4,5}(\mathrm{VB}) \rightarrow \Gamma_6(\mathrm{CB})$, as derived from the band structure computed by Chelikowsky and Cohen [17]. E_1 can be attributed to a transition to an impurity level 1.20 eV above the Γ_8(VB)

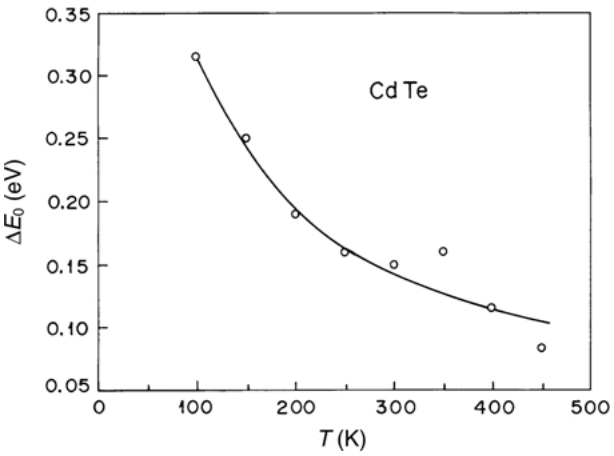

Figure 8 Dependence of $\Delta E_o (= E_o - E_g)$ on thermal treatment temperature for r.f. sputtered CdTe thin films. Solid line: calculated curve using Equation 11 (see text).

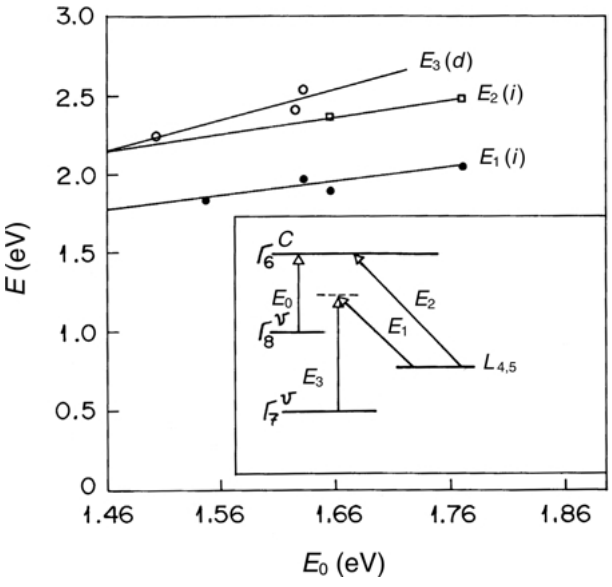

Figure 9 Transition energies for E_1, E_2, and E_3 as a function of E_o; inset: proposed interpretation for the four transitions. The superscripts v and c denote valence and conduction bands, respectively.

from the $L_{4,5}$(VB), situated at 0.65 eV below the Γ_8(VB) [17], (such a transition would have an energy equal to 2.09 eV close to $E_2 = 2.170 \pm 0.109$ eV). E_3 can be assigned to a transition to the same level from the Γ_7(VB) situated at 0.89 eV below the Γ_8(VB) (such a transition would have an energy equal to 1.85 eV, in agreement with the E_1 energy). The origin of such an impurity level may be associated with a native (e.g., Cd_i) or grain-boundary-related donor of depth 0.26 eV. A schematic diagram of the proposed transitions is given in the inset of Fig. 9.

4. Conclusion

CdTe thin films prepared by r.f. sputtering were found to be amorphous for $T_s \leq 200\,^{\circ}$C and polycrystalline for $T_s > 200\,^{\circ}$C. After annealing above 400 °C, the crystallites become visible in the SEM pictures (dimension 100–300 nm) and the luminescence band in the 5-K spectrum showed significant narrowing, suggesting that it involves transitions due to grain boundary defects. The refractive index n was determined from the interference pattern of the optical transmission. Both the values of n and its photon-energy dependence were found to agree satisfactorily with the Jensen theory for the refractive index of semiconductors below the bandgap. The dependence of the optical absorption on photon energy revealed the presence of four main allowed transitions, two of which are direct (E_o, E_3) and two are indirect (E_1, E_2). E_o and E_2 are attributed to transitions to the Γ_6(CB) from the Γ_8(VB) and $L_{4,5}$(VB), respectively. E_1 and E_3 are attributed to transitions to an impurity level situated at 1.20 eV above the Γ_8(VB) from the $L_{4,5}$(VB) and the Γ_7(VB), respectively.

Acknowledgments

The authors are grateful to Professor K. Herrmann for his help in luminescence measurements. The authors are also grateful to the Research Administration of Kuwait University for its financial support (project SP044).

References

1. T. L. CHU and S. S. CHU, *Prog. Photovolt.* **1** (1993) 31.
2. H. UDA, in ''II-VI Semiconductor Compounds'', edited by M. Jain (World Scientific, Singapore, 1993).
3. J. BRITT and C. FEREKIDES, *Appl. Phys. Lett.* **62** (1993) 2851.
4. A. COMPAAN, Private Communication, reported by NREL (May 2001).
5. P. M. AMIRTHARAJ, in ''Handbook of Optical Constants of Solids II'', edited by D. Palik (Academic, San Diego, 1991) p. 655.
6. S. S. OU, O. M. STAFSUDD and B. M. BASOL, *J. Appl. Phys.* **55** (1984) 3769.
7. A. E. RAKHSHANI, *ibid.* **81** (1997) 7988.
8. B. JENSEN, ''Handbook of Optical Constant of Solids'', Academic Press (1991) p. 125.
9. F. EL AKKAD, A. PUNNOOSE and G. PRABU, *Appl. Phys. A* **71** (2000) 157.
10. F. J. ESPINOZA-BELTRAN, F. SANCHEZ-SINENCIO, O. ZELA-ANGEL, J. G. MEDOZA-ALVAREZ, C. ALEJO-ARMENTA, C. VAZQUEZ-LOPEZ, M. H. FARIAS, G. SOTO, L. COTA-ARAIZA, J. L. PENA, J. A. AZAMAR-BARRIOS and L. BANOS, *Jpn. J. Appl. Phys.* **30** (1991) L1715.
11. F. J. ESPINOZA-BELTRAN, O. ZELAYA, F. SANCHEZ-SINENCIO, J. G. MEDOZA-ALVAREZ, M. H. FARIAS and L. BANOS, *J. Vac. Sci. Technol. A* **11**(6) (1993) 3062.
12. R. SWANEPOEL, *J. Phys. E. Sci. Instrum.* **16** (1983) 1214.
13. N. F. MOTT and E. A. DAVIS, ''Electronic Processes in Non-Crystalline Materials'' (Clarendon, Oxford, 1971) p. 238.
14. T. S. MOSS, ''Optical Properties of Solids'' (Butterworths, London, 1961) p. 34.
15. F. CERDEIRA, I. TORRIANO, P. MOTISUKE, V. LEMOS and F. DECKER, *Appl. Phys. A* **46** (1988) 107.
16. M. MELENDEZ-LIRA, S. JIMENES-SANDOVAL, I. HERNANDEZ-CALDERON, *J. Vac. Sci. Technol. A* **7** (1989) 1428.
17. J. R. CHELIKOWSKY and M. L. COHEN, *Phys. Rev. B* **14** (1976) 556.

Received 4 March
and accepted 2 September 2002